THE JOURNAL OF COMPARATIVE NEUROLOGY 474:589–602 (2004)

Subcellular and Subsynaptic Localization of Group I Metabotropic Glutamate Receptors in the Monkey Subthalamic Nucleus

MASAAKI KUWAJIMA,[1,2] RANDY A. HALL,[2] ATSU AIBA,[3] AND YOLAND SMITH[1,4]*
[1]Yerkes National Primate Research Center, Emory University, Atlanta, Georgia 30322
[2]Department of Pharmacology, Emory University School of Medicine, Atlanta, Georgia 30322
[3]Division of Cell Biology, Department of Molecular and Cellular Biology, Kobe University Graduate School of Medicine, 7-5-1 Kusunoki-cho, Chuo-ku, Kobe 650-0017, Japan
[4]Department of Neurology, Emory University School of Medicine, Atlanta, Georgia 30322

ABSTRACT

Both subtypes of group I metabotropic glutamate receptor, mGluR1 and mGluR5, are expressed postsynaptically in neurons of the subthalamic nucleus (STN), and their activation induces different physiological responses. To test whether these effects could be explained by a differential localization of the two group I mGluRs, we analyzed the subcellular and subsynaptic distribution of mGluR1a and mGluR5 in the monkey STN. Double-immunofluorescence and light microscopic analyses revealed that both group I mGluR subtypes were strongly coexpressed in the neuropil and neuronal perikarya. Astrocytic perikarya exhibited intense mGluR1a, but no detectable mGluR5, immunoreactivity. At the electron microscopic level, immunoperoxidase labeling for both mGluR1a and mGluR5 was localized mainly in dendrites. A significant proportion of the total pool of mGluR1a-immunoreactive elements was accounted for by glial cell processes, whereas glial cell labeling was much less frequently encountered in sections immunostained for mGluR5. Preembedding immunogold labeling in STN dendrites revealed that 60–70% of the gold labeling for both mGluR subtypes was intracellular, whereas 30–40% was apposed to the plasma membrane. Of the plasma membrane-apposed particles, more than 90% were extrasynaptic; fewer than 10% were associated with symmetric or asymmetric synapses. Most of the synapse-associated labeling was found at the edges of both asymmetric and symmetric postsynaptic specializations. Some extrasynaptic gold particles were aggregated on parts of the plasma membrane tightly apposed by glial processes. These findings demonstrate that mGluR1a and mGluR5 exhibit a similar pattern of subsynaptic localization in monkey STN neurons, with both receptor subtypes exhibiting substantial extrasynaptic and perisynaptic localization. J. Comp. Neurol. 474:589–602, 2004. © 2004 Wiley-Liss, Inc.

Indexing terms: basal ganglia; ultrastructure; immunogold method; GABA; glia

The subthalamic nucleus (STN) is a key component of the basal ganglia network that sends glutamatergic excitatory projections to the output nuclei of the basal ganglia, the substantia nigra pars reticulata (SNr) and internal globus pallidus (GPi; homologous to the entopeduncular nucleus in nonprimates; DeLong, 1990; Smith et al., 1998). A major pathophysiological feature following degeneration of the nigrostriatal dopaminergic projection in Parkinson's disease is an increased and/or burst firing activity of STN neurons and a resultant increase in neuronal activity of the basal ganglia output nuclei (Bergman et al., 1994). These observations have allowed for the recent development of highly effective surgical therapies, which are directed at reducing the increased basal ganglia

Grant sponsor: National Institutes of Health; Grant number: RR00165 (Yerkes Center); Grant number: R01-NS37423 (Y.S.); Grant number: R01-NS045644 (R.A.H.); Grant sponsor: the W.M. Keck Foundation/ Distinguished Young Scholar in Medical Research (R.A.H.).

*Correspondence to: Yoland Smith, Yerkes National Primate Research Center, Emory University, 954 Gatewood Rd. NE, Atlanta, GA 30329. E-mail: yolands@rmy.emory.edu

Received 16 April 2003; Revised 17 February 2004; Accepted 25 February 2004

DOI 10.1002/cne.20158

Published online in Wiley InterScience (www.interscience.wiley.com).

© 2004 WILEY-LISS, INC.

output by surgical ablation or high-frequency stimulation of STN (Bergman et al., 1990; Limousin et al., 1995). Elucidating the mechanisms that regulate excitability of STN neurons is, therefore, critical in understanding the role of STN in normal motor control and the pathophysiological changes that underlie Parkinson's disease.

Recent studies have suggested that metabotropic glutamate receptors (mGluRs) play important roles in regulating neuronal activity in basal ganglia nuclei including the STN. These receptors are a family of eight G-protein-coupled glutamate receptor subtypes that are classified into three groups based on their amino acid sequences, pharmacological profiles, and preferred second messenger pathways to which they are coupled (Nakanishi, 1992; Conn and Pin, 1997). Group I mGluRs include mGluRs 1 and 5, and their activation usually leads to phosphoinositide hydrolysis via $G_{q/11}$ and subsequent mobilization of intracellular Ca^{2+} and activation of protein kinase C (PKC). They could also mediate a decrease in K^+ conductance and an increase in Ca^{2+} conductance to modulate neuronal excitability (Conn and Pin, 1997). Group II (mGluRs 2 and 3) and group III (mGluRs 4, 6, 7, and 8) receptors are negatively coupled to adenylyl cyclase through $G_{i/o}$ and often mediate presynaptic inhibition of neurotransmitter release (Conn and Pin, 1997). Previous electron microscopic studies revealed that group I mGluRs are found at the edges of postsynaptic specializations at asymmetric glutamatergic synapses in the hippocampus and cerebellum (Baude et al., 1993; Nusser et al., 1994; Lujan et al., 1996) and various basal ganglia nuclei (Hanson and Smith, 1999; Hubert et al., 2001). We recently demonstrated that group I mGluRs are also found postsynaptically in the main body of GABAergic striatal synapses in both segments of the globus pallidus (GP; Hanson and Smith, 1999) and SNr (Hubert et al., 2001).

Neurons in the rat and monkey STN express both mGluR1 and mGluR5 proteins (Testa et al., 1998; Awad et al., 2000; Wang et al., 2000; Marino et al., 2002). An immunoperoxidase study at the electron microscopic level indicates that these receptors are mostly localized in postsynaptic dendrites of the rat STN, although a few presynaptic terminals were also labeled for mGluR1a (Awad et al., 2000). It was found that mGluR5, but not mGluR1, mediates slow excitatory responses and enhances N-methyl-D-aspartate (NMDA) receptor currents in rat STN neurons in slice preparations (Awad et al., 2000), but activation of both receptor subtypes mediates intracellular Ca^{2+} responses (Marino et al., 2002). In addition, mGluR1, along with group III mGluRs, mediates presynaptic inhibition of glutamate release (Awad-Granko and Conn, 2001).

The differential effects of the two group I mGluRs recorded in STN neurons appear to be a common phenomenon for most basal ganglia nuclei (Valenti et al., 2002). Knowing that the localization of receptors in relation to the synaptic sites of neurotransmitter release plays a major role in determining the physiological responses of postsynaptic neurons, one may hypothesize that the differential roles of mGluR1 and mGluR5 in STN neurons might potentially be accounted for by differences in receptor localization. Thus, the objective of the present study was to analyze the subcellular and subsynaptic localization of the two group I mGluRs in the monkey STN. Some of data presented in this paper have been published previously in abstract form (Kuwajima et al., 2001, 2002).

MATERIALS AND METHODS

Primary antibodies

The following commercially available antibodies were used to localize group I mGluRs: 1) affinity-purified polyclonal rabbit IgGs against carboxyl-terminal residues 1,180–1,199 of rat mGluR1a (0.5 μg/ml for immunocytochemistry; 0.04 μg/ml for Western immunoblots; Chemicon International, Temecula, CA); 2) monoclonal mouse IgGs against carboxyl-terminal residues 842–1,200 of human mGluR1a (1.0 μg/ml for immunocytochemistry; BD PharMingen, San Diego, CA; Petralia et al., 1997); and 3) affinity-purified polyclonal rabbit IgGs against carboxyl-terminal residues 1,152–1,171 of rat mGluR5 (0.86 μg/ml for immunocytochemistry; 0.17 μg/ml for Western immunoblots; Upstate Biotechnology, Lake Placid, NY). These antibodies were tested for their specificity with Western immunoblots and immunocytochemistry as described below. Specificity of the monoclonal mouse anti-mGluR1a antibody has been well characterized in previous studies (Petralia et al., 1997; Marino et al., 2001). For postembedding γ-aminobutyric acid (GABA) immunocytochemistry, polyclonal rabbit anti-GABA IgGs (1:1,000 dilution; Sigma, St. Louis, MO) were used.

Animals and tissue preparation

All procedures were approved by the animal care and use committees of Emory University and Kobe University and conformed to the U.S. National Institutes of Health guidelines. For immunocytochemistry, three adult rhesus monkeys (*Macaca mulatta*), one mGluR5-deficient mouse and one littermate wild-type mouse (The Jackson Laboratory, Bar Harbor, ME), and one mGluR1-deficient mouse (Aiba et al., 1994) and one littermate wild-type mouse were used. They were deeply anesthetized with an overdose of pentobarbital (100 mg/kg, i.v. for monkeys, i.p. for mice), and transcardially perfused with ice-cold oxygenated Ringer's solution, followed by a fixative solution containing 4.0% paraformaldehyde, 0.1–0.25% glutaraldehyde, and 0–0.2% picric acid in phosphate buffer (PB; 0.1 M; pH 7.4). The brain was then removed from the skull, blocked, and postfixed in the same fixative for 2 hours at 4°C before being washed in phosphate-buffered saline (PBS; 0.01 M; pH 7.4) and cut into 50–60-μm-thick coronal sections with a vibrating microtome.

For Western immunoblots, brain tissue from one rhesus monkey (*M. mulatta*), one Sprague-Dawley rat (Charles River Laboratories, Wilmington, MA), and one mGluR5-deficient mouse and one littermate wild-type mouse were used. The monkey was overdosed with pentobarbital (100 mg/kg, i.v.), followed by rapid removal of the brain from the skull and dissection. The rodents were rapidly decapitated, and the brain was removed from the skull and dissected on ice.

Western immunoblots

Human embryonic kidney (HEK-293) cells were maintained in complete medium (minimum essential medium with 10% fetal bovine serum and 1% penicillin/streptomycin) in 10-cm culture dishes at 37°C with 5% CO_2. The cells at ~50–80% confluence were transiently transfected with 2 μg of either mGluR1a or mGluR5b plasmid mixed with LipofectAmine (Invitrogen, Carlsbad, CA), followed by a 4-hr incubation at 37°C with 5% CO_2. After 6 ml of complete medium was added, the cells were

incubated for an additional 24 hr. The cells were then harvested in 1× SDS-PAGE sample buffer.

All brain membrane samples were prepared at 4°C. After dissection, the striatal tissue was completely homogenized with a sonicator in an ice-cold buffer solution containing 20 mM HEPES, 10 mM EDTA, and 2 mM Na_3VO_4. The homogenate was then centrifuged for 5 minutes at 2,000 rpm to remove tissue debris, and membranes were isolated from the supernatant by subsequent centrifugation for 30 minutes at 14,000 rpm. The resulting pellet was then solubilized in a buffer solution containing 20 mM HEPES and 0.1 mM EDTA before total protein concentration was measured by using the Bio-Rad Protein Assay (Bio-Rad, Hercules, CA). The homogenates were then centrifuged for 30 minutes at 14,000 rpm, and the pellet was solubilized in a lysis buffer containing 10 mM HEPES, 50 mM NaCl, 0.1 mM EDTA, 1 mM benzamidine, 1.0% Triton X-100, 0.1% SDS, and protease inhibitor cocktail (1 tablet per 50 ml; Roche Diagnostics GmbH, Mannheim, Germany). The lysates (50 μg protein) were then eluted with 6× SDS-PAGE sample buffer. The samples from transfected HEK-293 cells and brain tissue were resolved by SDS-PAGE and subjected to Western blot analysis with appropriate antibodies. Immunoreactive bands were detected with the enhanced chemiluminescence detection system (Pierce, Rockford, IL) with horseradish peroxidase-conjugated goat anti-rabbit secondary antibody (1:4,000; Amersham Biosciences, Little Chalfont, United Kingdom).

Double-immunofluorescence labeling of group I mGluRs

Sections containing STN were treated with 1.0% H_2O_2 in phosphate-buffered saline (PBS) for 10 minutes at room temperature (RT). The sections were then incubated for 1 hour at RT in PBS containing 5.0% normal donkey serum (NDS), 1.0% bovine serum albumin (BSA), and 0.3% Triton X-100, followed by the primary antibodies (mouse anti-mGluR1a and rabbit anti-mGluR5 IgGs) in a diluent solution containing 1.0% NDS, 1.0% BSA, and 0.3% Triton X-100 in PBS for 24 hours at RT. After PBS rinses, the sections were incubated for 1 hour in donkey anti-rabbit IgG conjugated with fluorescein and donkey anti-mouse IgG conjugated with rhodamine red (1:100 each; Jackson Immunoresearch Laboratories, West Grove, PA) diluted in the antibody diluent solution. The sections were then rinsed in PBS and incubated in a solution containing 10 mM $CuSO_4$ and 50 mM NH_4COOCH_3 at pH 5.0 for 30 minutes, followed by PBS rinses. They were mounted on glass slides, and coverslips were applied with Vectashield (Vector, Burlingame, CA). The mounted sections were stored in the dark at 4°C until examination with with a Zeiss LSM410 confocal microscope (Carl Zeiss MicroImaging, Inc., Thornwood, NY) with 510–525 nm and 575–640 nm bandpass emission filters for fluorescein and rhodamine, respectively. For analysis of group I mGluR colocalization, two tissue sections containing STN were used per animal (n = 2). The micrographs were then taken at random from the entire medial-lateral extent of the STN with a ×40 objective, and neuronal cell bodies immunopositive for mGluR1a, mGluR5, or both were counted. The pattern of group I mGluR distribution was the same for the medial-lateral extent of STN.

Immunoperoxidase localization of group I mGluRs for light microscopy

Tissue sections were treated with 1.0% $NaBH_4$ in PBS for 20 minutes at RT, followed by PBS rinses. The sections were then incubated for 1 hour at RT in PBS containing 10% normal goat serum (NGS), 1.0% BSA, and 0.3% Triton X-100, followed by the primary antibody solution containing 1.0% NGS, 1.0% BSA, and 0.3% Triton X-100 in PBS for 24 hours at RT. After PBS rinses, the sections were incubated for 90 minutes in biotinylated goat anti-rabbit IgG (1:200; Vector) diluted in the antibody diluent solution, followed by avidin-biotin-peroxidase complex (Vector). The sections were then washed in PBS and Tris buffer (50 mM; pH 7.6), and transferred to a solution containing 0.025% 3,3′-diaminobenzidine tetrahydrochloride (DAB; Sigma), 10 mM imidazole, and 0.005% hydrogen peroxide in Tris buffer for 10 minutes. After PBS washes, the sections were mounted on gelatin-coated slides and dehydrated, and a coverslip was applied with Permount. They were examined with a Leica DMRB microscope (Leica Microsystems, Inc., Bannockburn, IL), and images were acquired with a CCD camera (Leica DC500) controlled by Leica IM50 software (version 1.20).

Immunoperoxidase localization of group I mGluRs for electron microscopy

After $NaBH_4$ treatment, the sections were placed in a cryoprotectant solution for 20 minutes, followed by freeze-thawing as described previously (Hubert et al., 2001). The sections then underwent processing for the immunoperoxidase localization of group I mGluRs in a manner identical to that for light microscopy, except that the incubation with the primary antibodies was performed at 4°C for 48 hours, and Triton X-100 was omitted from all incubation solutions. After immunostaining, the sections were transferred to PB for 10 minutes and treated with 1.0% OsO_4 in PB for 20 minutes. They were then rinsed with PB and dehydrated in an ascending gradient of ethanol. Uranyl acetate (1.0%) was added to the 70% alcohol to enhance contrast. The sections were then treated with propylene oxide before being embedded in epoxy resin (Durcupan ACM; Fluka, Buchs, Switzerland) for 12 hours, mounted on microscope slides, and placed in the oven at 60°C for 48 hours. Samples of STN were then cut out from the slides, glued on the top of resin blocks with cyanoacrylate glue, and cut into 60-nm-thick ultrathin sections with an ultramicrotome (Leica Ultracut T2). The ultrathin sections were serially collected on single-slot Pioloform-coated copper grids, stained with lead citrate for 5 minutes, and examined with a Zeiss EM-10C electron microscope. The micrographs were acquired with 3.25- × 4-inch Kodak EM plates (printed on Ilford paper) or with a CCD camera (DualView 300W; Gatan, Inc., Pleasanton, CA) controlled by DigitalMicrograph software (version 3.6.5; Gatan, Inc.). Some digitally acquired micrographs were adjusted only for brightness and contrast, with the image resolution kept constant, with either DigitalMicrograph or Photoshop software (version 7.0; Adobe Systems, Inc., San Jose, CA) to optimize the quality of the images for analysis.

Preembedding immunogold localization of group I mGluRs

After freeze-thawing, sections processed for preembedding immunogold staining were incubated for 1 hour at RT

in a solution containing 10% NGS in PBS-BSA (0.005% BSA, 0.05% Tween 20, and 0.001% gelatin in PBS). The sections were then incubated with PBS-BSA containing 1% NGS and the primary antibodies for 48 hours at 4°C. After rinses in PBS-BSA, the sections were incubated for 2 hours at RT with goat anti-rabbit IgGs conjugated with 1.4-nm gold particles (1:100; Nanoprobes, Yaphank, NY) in PBS-BSA with 1% NGS. The sections were then fixed in 1% glutaraldehyde in PBS for 10 minutes at 4°C and rinsed with PB, followed by silver intensification of the gold particles with the HQ silver kit (Nanoprobes) for 5–10 minutes. They were then rinsed with PB and treated with 0.5–1.0% OsO_4 in PB for 10 minutes. The rest of the procedure was the same as that described above for the immunoperoxidase material.

Postembedding immunogold labeling of GABA

Some sections processed for preembedding immunogold staining for group I mGluRs were also processed for postembedding immunogold labeling for the neurotransmitter GABA. After 60-nm-thick sections were serially collected on single-slot Pioloform-coated gold grids, they were preincubated for 10 minutes in Tris-buffered saline (TBS; 50 mM; pH 7.6) containing 0.01% Triton X-100. This was followed by a 24-hour incubation at RT with the anti-GABA antibody diluted in TBS/Triton X-100. After the sections were washed in TBS/Triton X-100, followed by TBS (50 mM; pH 8.2), they were incubated with goat anti-rabbit IgG conjugated with 5-nm gold (1:50 in TBS 50 mM; pH 8.2; BBInternational, Cardiff, United Kingdom) for 90 minutes at RT. They were then washed with distilled water, stained with uranyl acetate (1% in distilled water) for 15 minutes, washed with distilled water, and stained with lead citrate before being examined in the electron microscope.

Control experiments

To control for nonspecific immunoreactivity, immunoblots and brain tissue sections were incubated with the primary antibodies omitted or preabsorbed with synthetic peptides containing the corresponding immunogen sequences (10 times the amount of the primary antibody by weight; Microchemical Facility, Winship Cancer Institute, Emory University School of Medicine), whereas the rest of the procedure remained the same as described above. For the immunoperoxidase procedure, tissue sections were also incubated in the absence of the primary and secondary antibodies to control for nonspecific staining by avidin-biotin-peroxidase complex. For immunofluorescence labeling, tissue sections were incubated with the mouse anti-mGluR1a, followed by anti-rabbit secondary antibodies, or with the rabbit anti-mGluR5, followed by anti-mouse secondary antibodies to control for cross-reactivity of the secondary antibodies. In addition, paraformaldehyde-fixed brain sections from mGluR1- and mGluR5-deficient mice were incubated for immunoperoxidase staining with their respective primary antibodies to confirm their specificity (Fig. 1C,F). These control incubations were performed in parallel with normal incubations and resulted in the total absence of immunoreactivity.

Analysis of material

The method of analysis employed for the electron microscopic examination in the present study was the same as that used in our previous studies (Hanson and Smith, 1999, 2002). In the sections processed for immunoperoxidase labeling, tissue was sampled randomly from two different animals for each group I mGluR subtype. Electron micrographs of STN were taken at ×10,000 and ×12,500 from ultrathin sections close enough to the surface of each section so that antibody penetration was optimal. All labeled elements in an area of observation were counted, and the total area of observation was measured to calculate densities of labeled elements. Any elements that were not identifiable because of lack of well-defined ultrastructural features were categorized as "unknown." These "unknown" elements most likely consisted predominantly of small-caliber dendrites, unmyelinated axons, and glial cell processes. Observations were made from a total area of 1,254.57 μm^2 of STN tissue from two animals immunostained for mGluR1a and 1359.48 μm^2 from two animals immunostained for mGluR5.

In the sections processed for preembedding immunogold labeling, electron micrographs of STN dendrites were taken at ×25,000, ×31,500, and ×40,000 from the surface of immunostained sections, where the labeling was optimal. The gold particles were then counted and classified into four categories (intracellular, synaptic, perisynaptic, and extrasynaptic) based on their localization in relation to the plasma membrane and postsynaptic densities visible in the plane of section (see Results for more details). Dendrites with poor ultrastructural preservation or cut in a plane of section that was not suitable to distinguish the pre- and postsynaptic membranes were omitted from the analysis. Some immunoreactive synapses were examined in at least three serial ultrathin sections to ascertain the specificity of labeling. Micrographs of gold-labeled dendrites were analyzed for total length of dendritic plasma membrane and total length of synaptic and perisynaptic plasma membrane by using the Neurolucida software (version 4.05c; MicroBrightField, Inc., Williston, VT). The mean size of gold particles was estimated by measuring the diameter of every gold particle in 10 randomly selected STN dendrites immunostained for the two group I mGluR subtypes in each animal.

RESULTS

Specificity of primary antibodies

As demonstrated previously in rat brain samples (Ferraguti et al., 1998; Testa et al., 1998; Marino et al., 2001), both affinity-purified polyclonal antibodies used in this study (i.e., anti-mGluR1a IgGs from Chemicon and anti-mGluR5 IgGs from Upstate) were found to be specific for their respective epitopes. Immunoblot analysis of transfected HEK-293 cell extracts showed that the anti-mGluR1a antibody recognized mGluR1a, with no detectable cross-reaction with mGluR5 (Fig. 1A). This antibody also labeled a single band in monkey and rat striatal membranes with an estimated molecular weight of approximately 140 kDa (Fig. 1A), which is consistent with a calculated molecular weight of ~133 kDa for mGluR1a (Houamed et al., 1991; Masu et al., 1991). This band was totally abolished when the antibody was preabsorbed with a synthetic peptide containing the corresponding antigen sequence (data not shown). In addition, immunoperoxidase staining for mGluR1a resulted in strong immunoreactivity in paraformaldehyde-fixed STN sections from

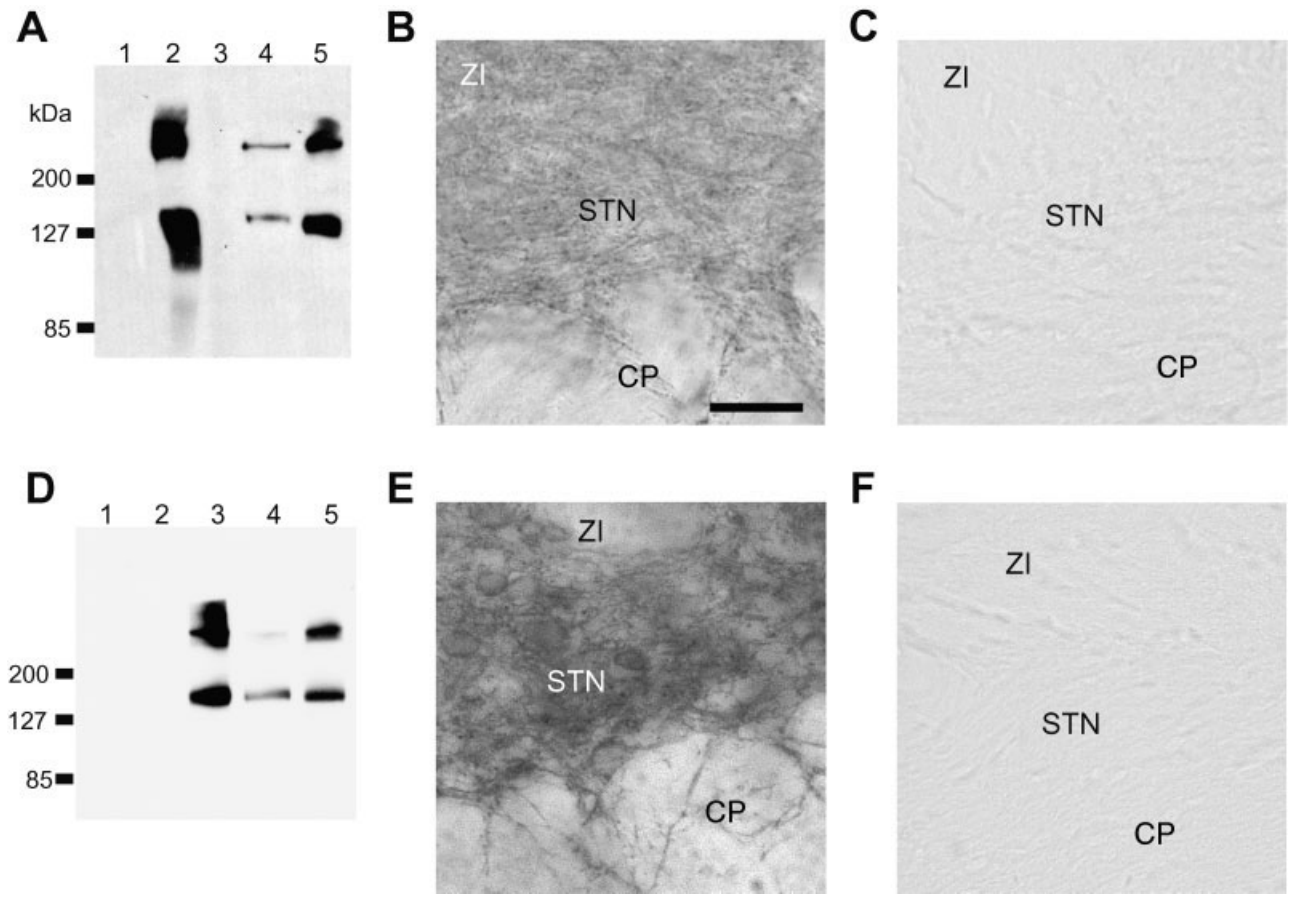

Fig. 1. Specificity of the polyclonal antibodies was tested by Western immunoblot and immunocytochemistry. **A,D:** Western immunoblot of HEK-293 cells transfected with no plasmid (lane 1), mGluR1a (lane 2), and mGluR5 (lane 3) as well as membrane samples (50 μg protein per lane) from the monkey putamen (lane 4) and the rat striatum (lane 5). A: The anti-mGluR1a antibody detected mGluR1a (lane 2) but not mGluR5 (lane 3). This antibody also detected a major band of about 140 kDa from the monkey and rat samples (lanes 4 and 5, respectively). D: The anti-mGluR5 antibody detected mGluR5 (lane 3) but not mGluR1a (lane 2). This antibody also detected a major band of about 140 kDa from the monkey and rat samples (lanes 4 and 5, respectively). **B,C:** Brain sections containing the subthalamic nucleus (STN) from wild-type (B) and mGluR1-deficient (C) mice were stained for mGluR1a by the immunoperoxidase method. In the wild-type mouse, strong mGluR1a ir was seen in cell bodies and neuropil in STN, whereas there was no detectable mGluR1a ir in the knockout tissue. **E,F:** Brain sections containing the STN from wild-type (E) and mGluR5-deficient (F) mice were stained for mGluR5 by the immunoperoxidase method. In the wild-type tissue, strong mGluR5 ir was found in neuropil and cell bodies in STN, whereas there was no detectable mGluR5 ir in the knockout tissue. CP, cerebral peduncle; ZI, zona incerta. Scale bar = 50 μm.

wild-type (Fig. 1B) but not mGluR1-deficient (Fig. 1C) mice. Immunoblot analysis of transfected HEK-293 cell extracts showed that the anti-mGluR5 antibody recognized only mGluR5, without any detectable cross-reactivity with mGluR1a (Fig. 1D). This antibody also labeled a single band in monkey and rat brain membranes with an estimated molecular weight of approximately 140 kDa (Fig. 1D), which is consistent with a calculated molecular weight of ~130 kDa for mGluR5 (Abe et al., 1992; Minakami et al., 1993). This band was totally absent in the brain membrane sample from mGluR5-deficient mouse (data not shown) and was totally abolished after the antibody was preabsorbed with the corresponding synthetic peptide (data not shown). Immunoperoxidase staining for mGluR5 resulted in strong immunoreactivity in paraformaldehyde-fixed STN sections from wild-type (Fig. 1E) but not mGluR5-deficient (Fig. 1F) mice. Furthermore, preabsorption of these antibodies also completely abolished staining during immunocytochemical procedures (data not shown).

Double-immunofluorescence and light microscopic observations

Double-immunofluorescence confocal microscopic observation of mGluR1a and mGluR5 in the monkey STN revealed coexpression of immunoreactivity (ir) for both group I mGluR subtypes in neuronal cell bodies and neuropil elements. Putative astrocytic cell bodies contained strong mGluR1a ir, whereas they did not display significant mGluR5 ir (Fig. 2). In contrast, most neurons exhibited strong ir for both mGluR1a and mGluR5. Among 218 STN neuronal cell bodies examined from two monkeys, 211 were immunoreactive for both group I mGluR subtypes. Three neurons were found to express only mGluR1a, but four were labeled only for mGluR5. At the light microscopic level with the immunoperoxidase

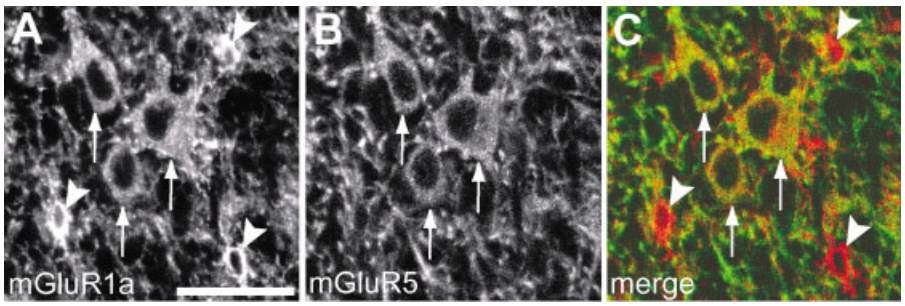

Fig. 2. **A–C:** Double-immunofluorescence labeling reveals coexpression of mGluR1a and mGluR5 immunoreactivity in monkey STN neurons. The arrows indicate double-labeled neuronal perikarya. The arrowheads point to putative astrocytes labeled for mGluR1a but not mGluR5. Note also the coexpression of mGluR1a and mGluR5 in neuropil elements. Scale bar = 50 μm.

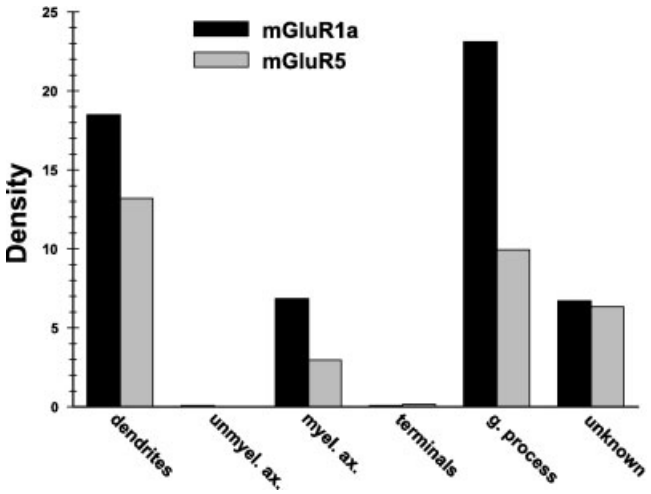

Fig. 3. Histogram comparing the density of mGluR1a and mGluR5 immunoperoxidase-labeled elements per 100 μm^2 of STN tissue. Note that most neuronal mGluR1a and mGluR5 immunoreactivity is found in postsynaptic dendrites, whereas very few presynaptic axon terminals contain immunoreactivity for either group I mGluR subtype. The density of mGluR5-immunopositive glial processes is substantially lower than that of mGluR1a-positive processes. Unmyel. ax., unmyelinated axons; myel. ax., myelinated axons; terminals, axon terminals; g. process, glial cell processes.

method, both group I mGluR subtypes exhibited a pattern of immunoreactivity consistent with the immunofluorescence observations; i.e., strong labeling for mGluR1a and mGluR5 (see Figs. 4A and 5A, respectively) was seen in neuropil and perikarya. Immunolabeling for mGluR1a was also seen in small cell bodies with multiple processes, which most likely correspond to astrocytes. The pattern and intensity of labeling for both mGluR1a and mGluR5 were the same throughout the entire extent of STN.

Electron microscopic observations

At the electron microscopic level, immunoperoxidase labeling for both mGluR1a and mGluR5 was localized mostly in postsynaptic dendritic processes (Figs. 3, 4B, 5B). Occasionally, thin, spine-like appendages emerging from labeled dendrites also displayed moderate immunoreactivity (Fig. 4B). STN dendrites and terminal boutons were often surrounded by glial processes, which contained a moderate to strong level of mGluR1a ir (Fig. 4C). The density of mGluR5-immunopositive glial processes was substantially lower than that of mGluR1a-positive processes (Fig. 3). Perikarya of STN neurons also contained immunoreactivity for both group I mGluR subtypes, which was often associated with the endoplasmic reticulum and Golgi apparatus. Small numbers of myelinated axons were weakly labeled for either receptor subtypes, whereas very few presynaptic terminals displayed group I mGluRs immunoreactivity (Fig. 3). There was no marked difference in the distribution pattern of the two group I mGluR subtypes in STN as detected by this method, except that the density of immunolabeled glial processes was higher in the tissue immunostained for mGluR1a than mGluR5 (Fig. 3).

Because of its diffuse and amorphous nature, the immunoperoxidase reaction product does not reveal the exact subsynaptic localization of receptors. To address this issue, we used the preembedding immunogold method at the electron microscopic level, an approach that offers a much higher level of spatial resolution. To study the relationships between the synaptic specializations and the localization of group I mGluR subtypes, micrographs of immunoreactive dendrites were taken in the STN. The gold particles that were apposed to or within 20 nm from the plasma membrane were classified as "plasma membrane-bound" and pooled into three categories (i.e., synaptic, perisynaptic, and extrasynaptic) based on their localization relative to postsynaptic specializations. The term "synaptic" is used to describe gold particles found within or apposed to the main body of postsynaptic specializations, whereas "perisynaptic" refers to regions of the plasma membrane within 20 nm from the edges of postsynaptic specializations. All other plasma membrane-bound gold particles were categorized as "extrasynaptic." The gold particles that were located more than 20 nm away from the plasma membrane were categorized as "intracellular." The 20-nm cutoff point was chosen based on the assertion that the distance between the epitope and the gold particle, bridged by the primary and secondary antibodies, can be approximately 20 nm (Blackstad et al., 1990).

There was no marked difference in the subcellular and subsynaptic distribution patterns of mGluR1a and mGluR5 ir in STN dendrites. Most gold particles associ-

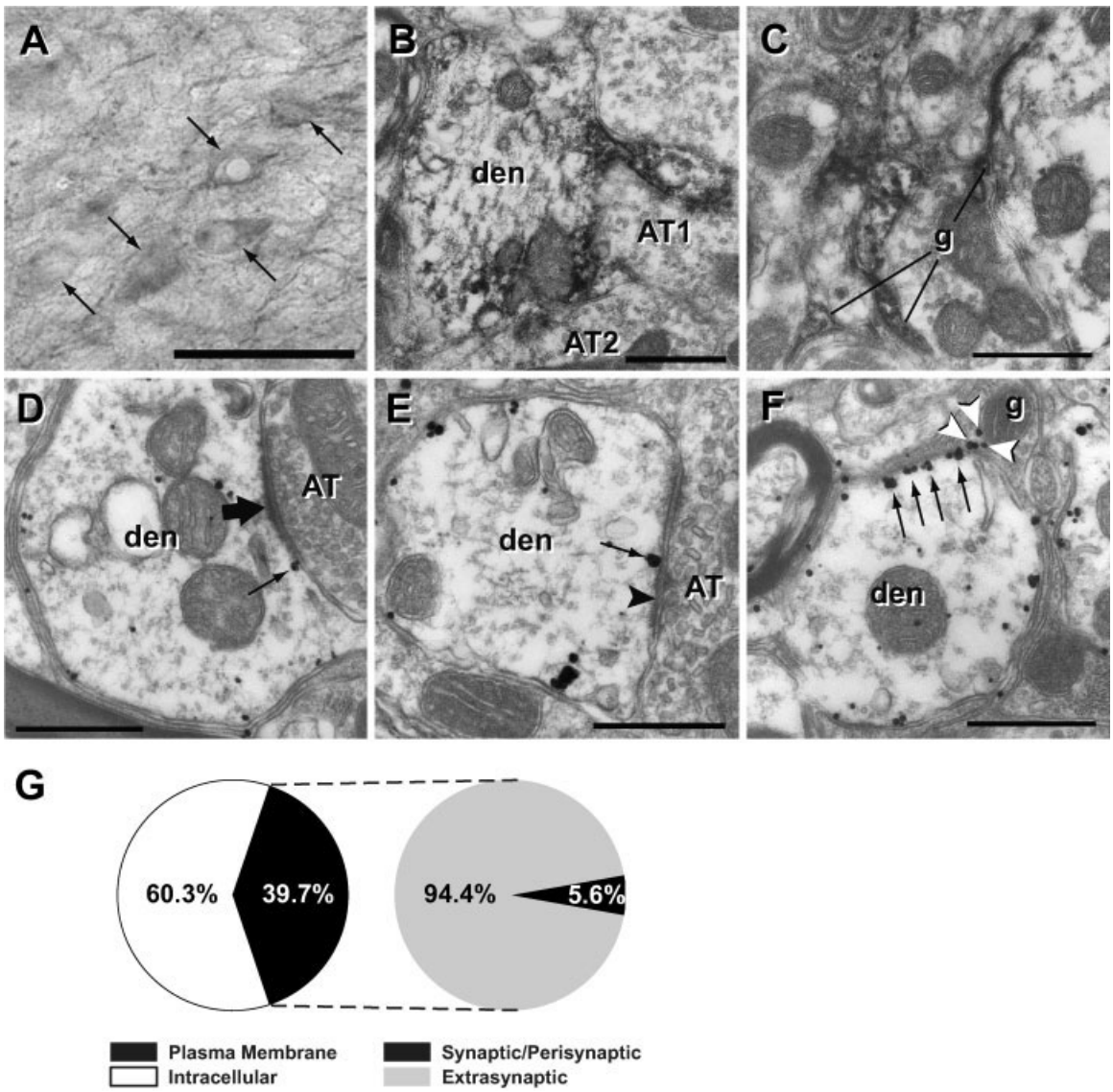

Fig. 4. Distribution of mGluR1a immunoreactivity in the monkey STN. **A:** Immunoperoxidase labeling for mGluR1a in STN at the light microscopic level shows densely stained neuropil and perikarya (arrows). **B:** A dendrite (den) immunopositive for mGluR1a is apposed by two axon terminals (AT1 and AT2). **C:** Glial processes (g) in STN also express mGluR1a. **D:** Electron micrograph of an asymmetric synapse (large arrow), showing perisynaptic immunogold labeling for mGluR1a (small arrow). Note that the bulk of mGluR1a labeling is localized intracellularly. **E:** Electron micrograph of a symmetric synapse (arrowhead), showing perisynaptic immunogold labeling for mGluR1a (arrow). **F:** Electron micrograph of an STN dendrite (den) showing clustering of mGluR1a immunolabeling on parts of the plasma membrane tightly apposed to glial processes (g), which also contain mGluR1a immunolabeling (arrowheads). **G:** Relative proportion of intracellular vs. plasma membrane-bound gold labeling for mGluR1a in STN dendrites (left) and extrasynaptic vs. synaptic/perisynaptic gold particles on the dendritic plasma membrane (right). In total, 2,595 gold particles in 277 STN dendrites from two animals were examined. Scale bars = 100 μm in A, 0.5 μm in B–F.

ated with both group I mGluR subtypes were localized intracellularly (Figs. 4G, 5G; 60.3% of total gold particles for mGluR1a and 70.1% for mGluR5), whereas about 30–40% were apposed to the plasma membrane. Of the plasma membrane-bound ir, more than 90% was extrasynaptic (Figs. 4G, 5G; 94.4% of all membrane-bound gold particles for mGluR1a and 92.6% for mGluR5). For both group I mGluR subtypes, most immunogold particles associated with postsynaptic specializations were found perisynaptically at both symmetric and asymmetric synapses, whereas only a low level of immunoreactivity was seen within the main body of the postsynaptic specializations (Figs. 5C, 6). Although it was not quantified, immunogold particle labeling for both group I mGluR subtypes was also observed in glial processes (Figs. 4F, 5C,D).

To ensure that the labeling at symmetric synapses was not an artifact of a random distribution of gold particles along the plasma membrane of STN dendrites, two further analyses were performed. First, we examined immunoreactive synapses through serial sections and found that

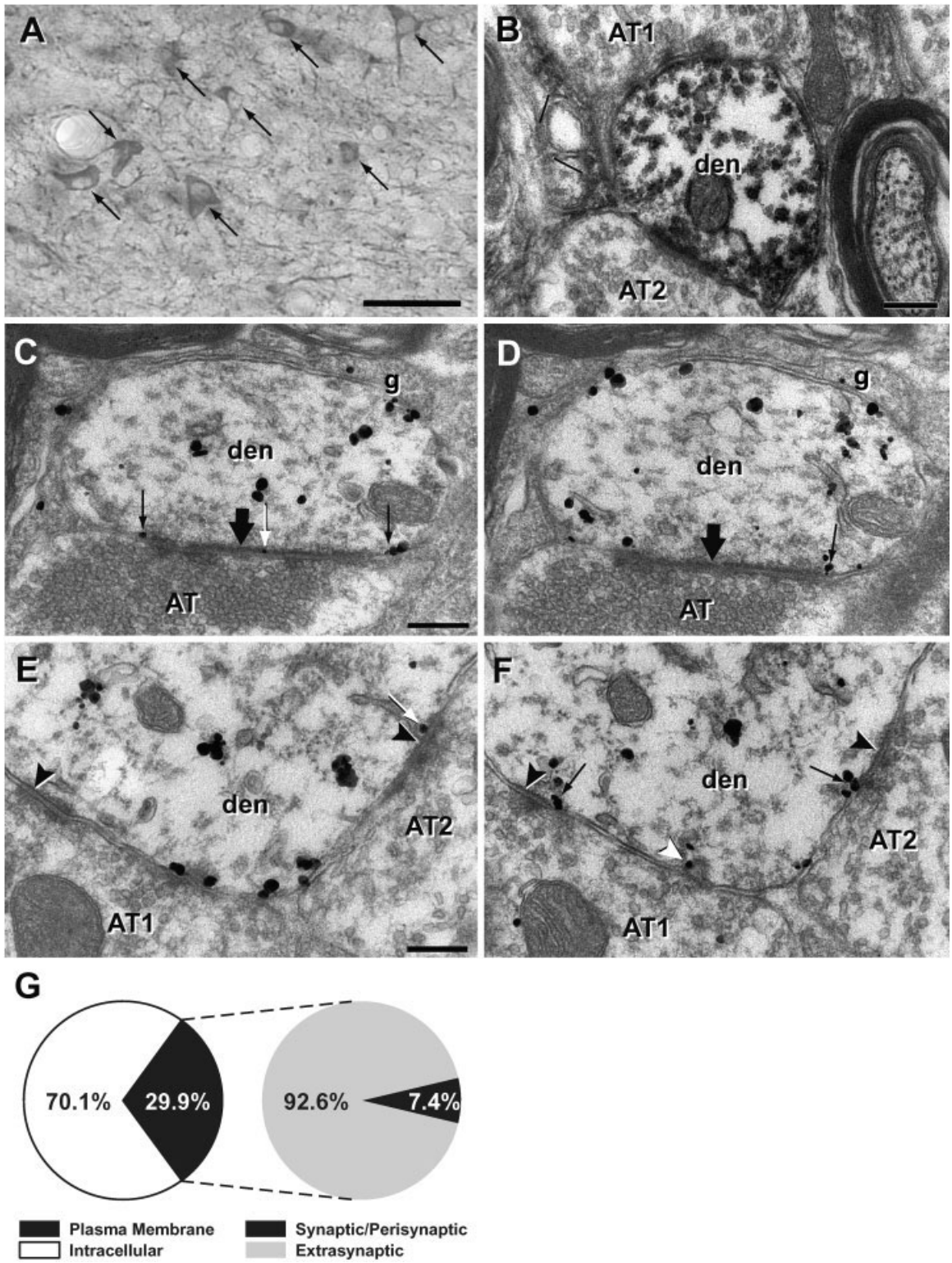

Fig. 5. Distribution of mGluR5 immunoreactivity in the monkey STN. **A:** Immunoperoxidase labeling for mGluR5 at the light microscopic level shows densely stained neuropil and perikarya (arrows). **B:** Glial processes (g) and dendrites (den) are labeled for mGluR5. The mGluR5-positive dendrite is contacted by two axon terminals (AT1 and AT2). **C,D:** Serial ultrathin sections of an asymmetric synapse (large black arrow), showing perisynaptic immunogold labeling for mGluR5 (small black arrows). These sections are 60 nm apart, indicating that multiple immunogold particles contribute to mGluR5 labeling at this synapse. Immunolabeling for mGluR5 is also present within the postsynaptic density (C; small white arrow) and in glial processes (g). Note that the bulk of mGluR5 labeling is localized intracellularly. **E,F:** Serial ultrathin sections of symmetric synapses (black arrowheads), showing perisynaptic (black arrows) and synaptic (white arrows) immunogold labeling for mGluR5. Note the immunolabeling associated with a coated pit-like indentation in the postsynaptic dendrite (F; white arrowhead). **G:** Relative proportion of intracellular vs. plasma membrane-bound gold particles for mGluR5 in STN dendrites (left) and extrasynaptic vs. synaptic/perisynaptic gold particles on the dendritic plasma membrane (right). These data were gathered from the analysis of 3,433 gold particles in 281 STN dendrites from two animals. Scale bars = 100 μm in A, 0.2 μm in B; bar in C = 0.2 μm for C,D; bar in E = 0.2 μm for E,F.

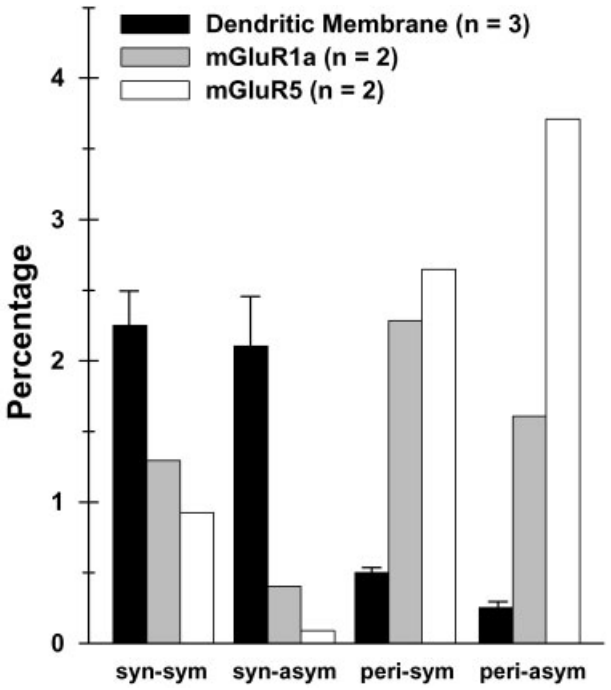

Fig. 6. Proportion of the dendritic plasma membrane involved in synapse formation was compared with the average percentage of plasma membrane-bound gold particles at symmetric and asymmetric synapses. The black bars indicate the percentage (mean ± SEM) of the dendritic plasma membrane contributing to synaptic (syn) and perisynaptic (peri) portions of symmetric (sym) and asymmetric (asym) synapses. Shown in gray and white bars are the average percentages of gold particles associated with each portion of dendritic membrane for mGluR1a and mGluR5, respectively. The total length of synaptic and perisynaptic plasma membrane was measured from 558 randomly selected STN dendrites from three animals. The percentages of synaptic and perisynaptic gold particles for group I mGluRs are the averages of mGluR1a and mGluR5 labeling in two animals each. Note that the proportion of group I mGluR labeling found within the main body of symmetric and asymmetric synapses (syn-sym and syn-asym, respectively) is substantially lower than the percentage of dendritic plasma membrane contributing to the formation of these regions. In contrast, the proportion of perisynaptic group I mGluR labeling at symmetric and asymmetric synapses (peri-sym and peri-asym, respectively) is at least 4.5-fold higher than the percentage of perisynaptic plasma membrane adjacent to symmetric and asymmetric synapses, suggesting preferential concentration of the receptors at perisynaptic sites along the plasma membrane of STN neurons.

immunoreactivity was maintained in three to five serial sections (Fig. 5C–F). Because the mean diameter of the silver-enhanced gold particles was 33.77 ± 0.69 nm (mean ± SEM; n = 365), an individual particle could not be found in more than two adjacent ultrathin (60-nm-thick) sections. Therefore, because some symmetric synapses were labeled in as many as five serial sections, multiple gold particles must have contributed to the immunolabeling. Second, we calculated the predicted percentage of gold particles found at synapses based on a random distribution on the dendritic plasma membrane. This was achieved by comparing the percentage of gold particles associated with synaptic and perisynaptic membrane with the proportion of the surface of the dendritic plasma membrane involved in these microdomains. We examined a total of 558 randomly selected STN dendrites from three animals and found that approximately 2% of the dendritic plasma membrane contributed to either symmetric or asymmetric synapses (i.e., along postsynaptic specializations), whereas under 1% accounted for the perisynaptic plasma membrane (i.e., 20 nm from the edges of postsynaptic specializations) at symmetric or asymmetric synapses (Fig. 6, black bars). If the plasma membrane-bound receptor immunoreactivity was randomly distributed, one would expect to find percentages of immunogold particles associated with synaptic and perisynaptic membrane in the same range as that revealed by random plasma membrane measurements. Contrary to this assumption, the percentage of perisynaptic immunolabeling adjacent to symmetric and asymmetric synapses for both group I mGluR subtypes was at least 4.5-fold higher than would be expected based on a random distribution (Fig. 6, peri-sym and peri-asym). On the other hand, the occurrence of both mGluR1a and mGluR5 labeling within the postsynaptic specializations of symmetric and asymmetric synapses was substantially lower than would be expected from a random distribution (Fig. 6, syn-sym and syn-asym). Postembedding immunocytochemistry confirmed that axon terminals forming the symmetric synapses labeled for mGluR1a or mGluR5 displayed GABA ir (Fig. 7A,C,D), whereas perisynaptically labeled asymmetric synapses were formed by GABA-negative terminals (Fig. 7B,C).

DISCUSSION

The main finding of this study is that the two group I mGluR subtypes, mGluR1a and mGluR5, display a similar pattern of subcellular and subsynaptic distribution in the monkey STN, unlike the case in the SNr and the striatum, where specific features differentiated the localization of these two receptor subtypes (Hubert et al., 2001; Paquet and Smith, 2003). Interestingly, mGluR5, but not mGluR1, mediates slow depolarization and enhances NMDA currents in rat STN neurons (Awad et al., 2000). However, activation of both group I mGluR subtypes induces intracellular Ca^{2+} response in these cells (Marino et al., 2002). Thus, based on our observations, it seems unlikely that the differential physiological responses induced by mGluR1 and mGluR5 on STN neurons can be explained by a differential subcellular localization of the two receptor subtypes. It is noteworthy that complex interactions between mGluR1 and mGluR5 were also demonstrated in other basal ganglia nuclei, including the SNr (Marino et al., 2001, 2002) and GP (Poisik et al., 2003). Together, these findings indicate that the two group I mGluRs display a highly specific pattern of distribution and mediate differential effects whenever they coexist in individual basal ganglia neurons (Valenti et al., 2002).

Another important finding of our study is that group I mGluRs are concentrated perisynaptically not only at the postsynaptic specializations of asymmetric synapses but also at symmetric synapses established by GABA-immunoreactive putative pallidal terminals in the monkey STN (Figs. 6, 7). The ultrastructural features, large size, and pattern of innervation of STN neurons by these GABAergic terminal boutons are consistent with those of terminals from the external GP (GPe) described in previous studies (Shink et al., 1996). The pattern of group I mGluR distribution in the STN is markedly different from

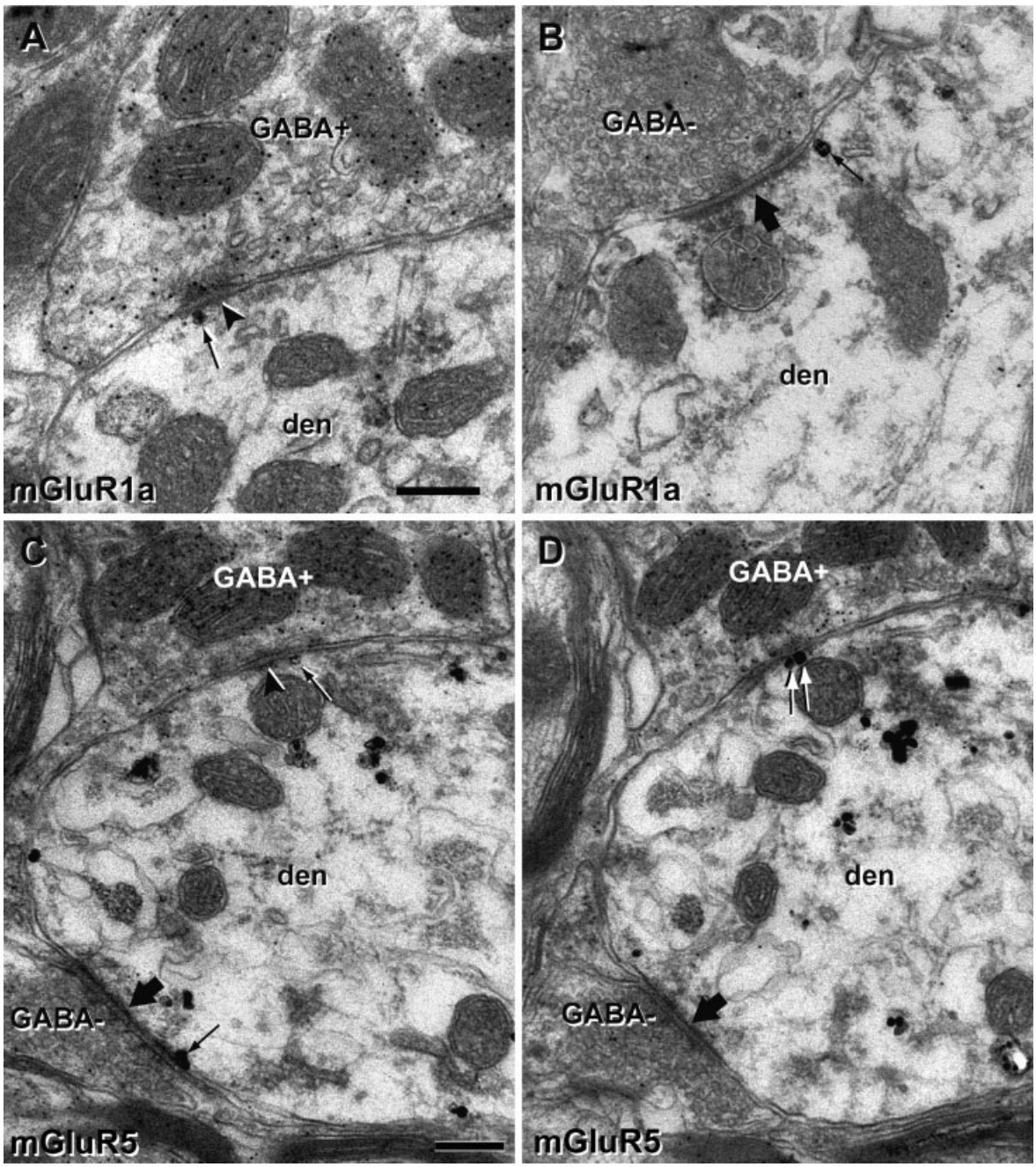

Fig. 7. Group I mGluRs are localized postsynaptic to GABA-immunoreactive terminal boutons. **A:** mGluR1a immunolabeling (arrow) is apposed to the postsynaptic specialization of a symmetric synapse (arrowhead) formed by a GABA-immunoreactive terminal ($GABA^+$). **B:** mGluR1a ir (small arrow) is localized at the edge of the postsynaptic specialization of an asymmetric synapse (large arrow) formed by a non-GABA immunoreactive terminal ($GABA^-$). **C,D:** Serial sections of a mGluR5-immunoreactive dendrite that displays perisynaptic labeling (small arrows in C) at a symmetric synapse (arrowhead in C) formed by a GABA-containing terminal ($GABA^+$) and at an asymmetric synapse (large arrows in C,D) formed by a GABA-negative bouton ($GABA^-$). In D, silver-enhanced gold particles (small arrows in D) are attached to parts of the plasma membrane corresponding to the site of synaptic specialization shown in C, but the plane of section does not allow us to assess the precise subsynaptic localization of this labeling. Scale bar in A = 0.2 μm for A,B; bar in C = 0.2 μm for C,D.

that in the hippocampus and cerebellum, where these receptors are found perisynaptically at asymmetric synapses without any substantial association with symmetric synapses (Nusser et al., 1994; Lujan et al., 1996). Previous studies from our laboratory found group I mGluRs in the main body of symmetric synapses established by putative GABAergic striatal terminals in the GP (Hanson and Smith, 1999) and the SNr (Hubert et al., 2001). Such a

mismatch between receptor localization and presynaptic neurotransmitter content is not unique to group I mGluRs. For example, immunolabeling for NR1 and GluR2/3 subunits of ionotropic glutamate receptors has been found postsynaptic to GABA-immunopositive pallidosubthalamic terminals in rats (Clarke and Bolam, 1998). Since STN dendrites are contacted by numerous GABAergic pallidal terminal boutons, it could be argued that our data indicate immunolabeling that is nonspecific, coincidental, or due to cross-reaction of the primary antibodies with $GABA_B$ receptors. This is, however, highly unlikely based on a number of observations. 1) The two polyclonal primary antibodies used in this study were found to be highly specific for their corresponding epitopes in immunocytochemical analyses with the knockout tissues (Fig. 1C,F) as well as in Western immunoblot analyses in this study (Fig. 1A,D) and previous studies (Ferraguti et al., 1998; Testa et al., 1998; Marino et al., 2001). 2) $GABA_B$ receptors do not contain amino acid sequences similar to the antigens that were used to raise the anti-mGluR1a and anti-mGluR5 antibodies (Kaupmann et al., 1997, 1998; Jones et al., 1998; White et al., 1998). 3) Omission or preabsorption of the primary antibodies resulted in the complete absence of immunostaining (data not shown). 4) Immunolabeling at individual symmetric synapses was found in up to five serial sections (Fig. 5C–F). 5) The proportion of plasma membrane-bound gold particles found perisynaptically at symmetric synapses was at least 4.5-fold higher than would be expected based on a random distribution (Fig. 6). Therefore, our data demonstrate that group I mGluRs are preferentially expressed perisynaptically at symmetric and asymmetric synapses in the monkey STN.

Because postsynaptic specializations at asymmetric synapses are made up of a highly dense and complex matrix of proteins (Choquet and Triller, 2003), one could argue that the scarce immunogold labeling associated with the main body of postsynaptic densities may be due to the inability of primary antibodies to reach their epitopes, rather than indicating the genuine lack of synaptic receptors. Although we cannot rule out that some group I mGluRs may, indeed, be expressed at synapses, various lines of direct and indirect evidence suggest their peri- and extrasynaptic localization. 1) Group I mGluRs were also found at perisynaptic and extrasynaptic sites in hippocampal and cerebellar tissue processed with the postembedding immunogold method (Nusser et al., 1994; Lujan et al., 1997; Petralia et al., 2001), an approach that overcomes the problem inherent to limited penetration of antibodies through thick sections used for preembedding immunocytochemistry. 2) Previous preembedding immunogold studies demonstrated that these receptors are found within the main body of postsynaptic specializations at symmetric synapses in the GP (Hanson and Smith, 1999) and SNr (Hubert et al., 2001). 3) Postsynaptic group I mGluR responses necessitate tetanic stimulation of glutamatergic afferents, and rely upon glutamate reuptake mechanisms (Batchelor et al., 1994; Tempia et al., 1998; Brasnjo and Otis, 2001; Reichelt and Knopfel, 2002), indicating that extrasynaptic glutamate spillover may be the main source of group I mGluR activation. It is noteworthy that many G-protein-coupled receptors, including D1 and D2 dopamine receptors (Yung et al., 1995), m4 muscarinic acetylcholine receptors (Bernard et al., 1999), μ-opioid receptors (Gracy et al., 1997), and somatostatin 2A receptors (Dournaud et al., 1998), are expressed along nonsynaptic sites of the neuronal plasma membrane, which suggests that the slow modulatory effects mediated by these receptors are largely dependent on extrasynaptic spillover and/or nonsynaptic release of neurotransmitters.

As previously pointed out (Hanson and Smith, 1999; Hubert et al., 2001), the main issue that remains is to find out the potential sources of glutamate that could activate group I mGluRs at GABAergic synapses and extrasynaptic sites. As mentioned above, one possibility is that these receptors are activated by glutamate spilled over from the synaptic cleft of neighboring glutamatergic synapses. It has been demonstrated previously that glutamate can, indeed, diffuse away from synapses and activate neighboring ionotropic glutamate receptors in the hippocampus (Asztely et al., 1997; Barbour and Hausser, 1997). Insofar as group I mGluRs have higher glutamate binding affinity than AMPA/kainate receptors (Conn and Pin, 1997; Dingledine et al., 1999), there is a strong possibility that glutamate spillover may activate group I mGluRs at GABAergic synapses and extrasynaptic sites. Another possibility is the nonsynaptic release of glutamate from astrocytes (Araque et al., 1999). There is, indeed, growing evidence that astrocytes act as active participants in the regulation of neuronal activity and synaptic transmission in the CNS (Araque et al., 1999). In fact, astrocytes can release glutamate in response to electrical or mechanical stimulation (Araque et al., 1998) and waves of elevated intracellular Ca^{2+} (Parpura et al., 1994). It is noteworthy that we found extrasynaptic mGluR1a ir associated with parts of the plasma membrane of STN dendrites tightly contacted by glial processes (Fig. 4G). A third possibility is that pallidal terminals in the STN corelease GABA and glutamate. Terminal boutons from GPe express a significantly higher level of glutamate ir than GABAergic striatopallidal terminals in the monkey GPi (Shink and Smith, 1995). GPe projections to GPi are largely made up of axon collaterals from the pallidosubthalamic projections (Sato et al., 2000), so it is reasonable to believe that GPe terminals in the STN are also enriched in glutamate ir. However, there is no direct evidence suggesting that GPe terminals release glutamate in the STN. Although corelease of fast neurotransmitters such as glutamate and GABA is not commonly observed in the central nervous system, it has been clearly demonstrated that the fast neurotransmitters glycine and GABA are coreleased from certain central synapses (Jonas et al., 1998). Furthermore, Walker et al. (2001) demonstrated monosynaptic $GABA_A$ receptor-mediated synaptic currents at glutamatergic mossy fiber-CA3 synapses in the hippocampus. Mossy fiber terminals, which are known to be glutamatergic, also exhibit intense GABA ir (Sandler and Smith, 1991; Sloviter et al., 1996) and express GAD67, a GABA-synthesizing enzyme (Sloviter et al., 1996). Future studies with vesicular glutamate transporters as markers of glutamatergic terminals should be conducted to assess whether GPe terminals are, indeed, capable of packaging glutamate into synaptic vesicles and possibly using it as neurotransmitter.

Assuming that group I mGluRs are activated at GABAergic synapses and extrasynaptic sites, one may wonder about the potential roles of these receptors at nonglutamatergic sites. Based on findings in other brain regions, it could be hypothesized that group I mGluRs expressed at GABAergic synapses modulate GABA

receptor-mediated responses via mobilization of intracellular Ca^{2+} and activation of protein kinase C (PKC). For instance, Hoffpauir and Gleason (2002) demonstrated that activation of mGluR5 enhances $GABA_A$-mediated currents in a Ca^{2+}- and PKC-dependent manner in retinal amacrine cells. In addition, the carboxyl-terminal tail of $GABA_B$ receptors contains consensus sites for PKC phosphorylation, which can suppress $GABA_B$ receptor-mediated K^+ conductance in hippocampus (for review see Couve et al., 2000). Although such interactions between group I mGluRs and GABA receptors have not been demonstrated in STN neurons, these observations, combined with the fact that both $GABA_A$ and $GABA_B$ receptors are strongly expressed in these neurons (Smith et al., 2001), suggest that activation of group I mGluRs could modulate GABA receptor signaling via PKC-mediated receptor phosphorylation in the monkey STN.

We also found that most group I mGluR labeling was localized intracellularly in STN dendrites. Since some immunolabeling was associated with microtubules and intracellular organelles such as the endoplasmic reticulum, this may represent receptors in the process of trafficking to the plasma membrane. Because the ligand binding domain of group I mGluRs is located in the extracellular amino-terminal region (Conn and Pin, 1997), these receptors must be inserted in the plasma membrane to be functional. Recent studies in cultured mammalian cells and neurons suggest that the trafficking of group I mGluRs to the cell surface is regulated by a family of cytoplasmic adaptor proteins called "Homer" (for reviews see Xiao et al., 2000; De Bartolomeis and Iasevoli, 2003). For example, in cultured cerebellar granule cells, transfection of Homer 1b induced intracellular retention of transfected mGluR5, whereas the subsequent induction of Homer 1a by application of NMDA and kainate caused the receptor to be trafficked to synaptic membranes (Ango et al., 2002). It is, therefore, conceivable that the relative abundance of group I mGluRs on the plasma membrane of STN neurons could be regulated in an activity-dependent manner via the expression of Homer 1a protein. Another possibility is that at least some intracellular labeling for group I mGluRs represents internalized receptors in the process of desensitization. Indeed, prolonged agonist stimulation is known to induce the internalization of group I mGluRs in a manner dependent on G-protein-coupled receptor kinases (Dale et al., 2000), β-arrestin, and dynamin (Mundell et al., 2001). Consistently with this idea, we found some immunolabeling associated with putative coated pits in the plasma membrane of postsynaptic dendrites (Fig. 5F). Although β-arrestin can mediate activation of mitogen-activated protein kinase signaling cascades following receptor internalization (Pierce and Lefkowitz, 2001; Iacovelli et al., 2003), it is unknown whether such is the case for group I mGluRs in the STN.

Glial processes also contained immunoreactivity for both mGluR1a and mGluR5. Our observation of mGluR1a ir in glial processes was a rather surprising finding, considering the previous demonstrations that mGluRs 3 and 5 are the predominant mGluR subtypes expressed in rodent glial cells (Winder and Conn, 1996). It should be noted, however, that glial cells are heterogeneous with respect to brain areas (Wilkin et al., 1990), and it is conceivable that the pattern of mGluR expression may differ from one brain region to another. In fact, the white matter of the rat optic nerve (Jensen and Chiu, 1993) and cultured astrocytes from the rat spinal cord (Silva et al., 1999) have been shown to express mGluR1. It is also possible that our results indicate genuine species differences in the expression pattern of group I mGluRs in glial cells, because most previous studies on glial mGluRs have been conducted in rodents. Because we used three different immunocytochemical techniques [i.e., immunofluorescence (Fig. 2), immunoperoxidase (Fig. 4C), and preembedding gold (Fig. 4F)] with two highly specific antibodies, it is unlikely that the presence of mGluR1a in glial cell processes in the monkey STN is the result of nonspecific immunolabeling. While the astrocytic cell bodies contained little mGluR5 ir in Triton-treated tissue processed for immunofluorescence (Fig. 2B,C), glial processes clearly exhibited mGluR5 ir in Triton-untreated immunoperoxidase-stained tissue at the electron microscopic level (Figs. 3, 5B). Thus, it appears that mGluR5 in monkey STN astrocytes is expressed predominantly in their processes and not as much in the cell bodies. A growing body of evidence suggests that group I mGluRs expressed in glial cells are involved in intracellular signaling and glial function (e.g., Ca^{2+} mobilization and regulation of K^+ conductance; for a review see Winder and Conn, 1996).

Previous electrophysiological data showed that group I and group III mGluRs activation mediates presynaptic inhibition of glutamate release in the STN of young rats (Awad-Granko and Conn, 2001). However, very few presynaptic terminals display group I mGluRs ir in the adult rat STN (Awad et al., 2000). Similarly, the results of the present study demonstrate very scarce presynaptic group I mGluRs labeling in the monkey STN. It seems, therefore, unlikely that the presynaptic effects of group I mGluRs activation on glutamate neurotransmission are mediated solely by activation of presynaptic receptors. Recent data showed that activation of CB1 cannabinoid receptors mediates some of the presynaptic effects induced by group I mGluRs activation in the hippocampus and cerebellum (for review see Doherty and Dingledine, 2003). The fact that STN expresses cannabinoid receptors (Mailleux and Vanderhaeghen, 1992) suggests that a similar mechanism may be involved in this brain region.

It is well established that one of the main physiological changes that underlies Parkinson's disease pathophysiology is an increased and/or burst activity of STN neurons (DeLong, 1990). Because of its preponderance in the STN and throughout the basal ganglia circuitry, mGluR5 has become an interesting target for potential therapy in Parkinson's disease (Rouse et al., 2000). Data obtained so far are encouraging and demonstrate that, indeed, the highly specific mGluR5 antagonist methylphenylethynylpyridine (MPEP) has significant antiparkinsonian effects in 6-hydroxydopamine-treated rats (Breysse et al., 2002, 2003). It remains to be established whether these effects are mediated by the selective blockade of mGluR5 in the STN or other motor-related brain regions. Though still preliminary, these observations, combined with the high degree of heterogeneity in the distribution and function of mGluRs in the basal ganglia, pave the way for the development of novel therapeutic strategies for Parkinson's disease and other movement disorders.

In summary, the present study provides a detailed description of the subcellular and subsynaptic localization of group I mGluRs in the monkey STN. Our data demonstrate that the overall distribution pattern of these recep-

tors is similar. Both mGluR1a and mGluR5 are preferentially concentrated in the perisynaptic portions of dendritic plasma membrane adjacent to both asymmetric and symmetric, GABAergic, synapses. In addition, most plasma membrane-bound group I mGluRs are found at extrasynaptic sites, with some apposed to parts of the plasma membrane tightly contacted by glial cell processes. Although the actions of fast neurotransmitters such as glutamate have long been thought to be restricted to their release site at the synaptic junction, this complex pattern of subsynaptic localization of group I mGluRs, combined with various lines of evidence for extrasynaptic glutamate spillover in the CNS (Asztely et al., 1997; Barbour and Hausser, 1997), suggests that activation of nonsynaptic group I mGluRs may mediate complex modulatory responses in STN neuronal activity and intracellular signaling cascades.

ACKNOWLEDGMENTS

The authors thank Jean-François Paré, Susan Maxson, Kelly B. Philpot, Amanda M. Castleberry, and Anthony G. Lau for their technical assistance; Frank Kiernan for photography; Dr. Chris Muly for fresh monkey brain tissue; and Dr. Toshio Terashima for preparation of fixed brain tissue from mGluR1-deficient mice.

LITERATURE CITED

Abe T, Sugihara H, Nawa H, Shigemoto R, Mizuno N, Nakanishi S. 1992. Molecular characterization of a novel metabotropic glutamate receptor mGluR5 coupled to inositol phosphate/Ca^{2+} signal transduction. J Biol Chem 267:13361–13368.

Aiba A, Chen C, Herrup K, Rosenmund C, Stevens CF, Tonegawa S. 1994. Reduced hippocampal long-term potentiation and context-specific deficit in associative learning in mGluR1 mutant mice. Cell 79:365–375.

Ango F, Robbe D, Tu JC, Xiao B, Worley PF, Pin JP, Bockaert J, Fagni L. 2002. Homer-dependent cell surface expression of metabotropic glutamate receptor type 5 in neurons. Mol Cell Neurosci 20:323–329.

Araque A, Parpura V, Sanzgiri RP, Haydon PG. 1998. Glutamate-dependent astrocyte modulation of synaptic transmission between cultured hippocampal neurons. Eur J Neurosci 10:2129–2142.

Araque A, Parpura V, Sanzgiri RP, Haydon PG. 1999. Tripartite synapses: glia, the unacknowledged partner. Trends Neurosci 22:208–215.

Asztely F, Erdemli G, Kullmann DM. 1997. Extrasynaptic glutamate spillover in the hippocampus: dependence on temperature and the role of active glutamate uptake. Neuron 18:281–293.

Awad H, Hubert GW, Smith Y, Levey AI, Conn PJ. 2000. Activation of metabotropic glutamate receptor 5 has direct excitatory effects and potentiates NMDA receptor currents in neurons of the subthalamic nucleus. J Neurosci 20:7871–7879.

Awad-Granko H, Conn PJ. 2001. Activation of groups I or III metabotropic glutamate receptors inhibits excitatory transmission in the rat subthalamic nucleus. Neuropharmacology 41:32–41.

Barbour B, Hausser M. 1997. Intersynaptic diffusion of neurotransmitter. Trends Neurosci 20:377–384.

Batchelor AM, Madge DJ, Garthwaite J. 1994. Synaptic activation of metabotropic glutamate receptors in the parallel fibre-Purkinje cell pathway in rat cerebellar slices. Neuroscience 63:911–915.

Baude A, Nusser Z, Roberts JD, Mulvihill E, McIlhinney RA, Somogyi P. 1993. The metabotropic glutamate receptor (mGluR1 alpha) is concentrated at perisynaptic membrane of neuronal subpopulations as detected by immunogold reaction. Neuron 11:771–787.

Bergman H, Wichmann T, DeLong MR. 1990. Reversal of experimental parkinsonism by lesions of the subthalamic nucleus. Science 249:1436–1438.

Bergman H, Wichmann T, Karmon B, DeLong MR. 1994. The primate subthalamic nucleus. II. Neuronal activity in the MPTP model of parkinsonism. J Neurophysiol 72:507–520.

Bernard V, Levey AI, Bloch B. 1999. Regulation of the subcellular distribution of m4 muscarinic acetylcholine receptors in striatal neurons in vivo by the cholinergic environment: evidence for regulation of cell surface receptors by endogenous and exogenous stimulation. J Neurosci 19:10237–10249.

Blackstad TW, Karagulle T, Ottersen OP. 1990. MORFOREL, a computer program for two-dimensional analysis of micrographs of biological specimens, with emphasis on immunogold preparations. Comput Biol Med 20:15–34.

Brasnjo G, Otis TS. 2001. Neuronal glutamate transporters control activation of postsynaptic metabotropic glutamate receptors and influence cerebellar long-term depression. Neuron 31:607–616.

Breysse N, Baunez C, Spooren W, Gasparini F, Amalric M. 2002. Chronic but not acute treatment with a metabotropic glutamate 5 receptor antagonist reverses the akinetic deficits in a rat model of parkinsonism. J Neurosci 22:5669–5678.

Breysse N, Amalric M, Salin P. 2003. Metabotropic glutamate 5 receptor blockade alleviates akinesia by normalizing activity of selective basal-ganglia structures in parkinsonian rats. J Neurosci 23:8302–8309.

Choquet D, Triller A. 2003. The role of receptor diffusion in the organization of the postsynaptic membrane. Nat Rev Neurosci 4:251–265.

Clarke NP, Bolam JP. 1998. Distribution of glutamate receptor subunits at neurochemically characterized synapses in the entopeduncular nucleus and subthalamic nucleus of the rat. J Comp Neurol 397:403–420.

Conn PJ, Pin JP. 1997. Pharmacology and functions of metabotropic glutamate receptors. Annu Rev Pharmacol Toxicol 37:205–237.

Couve A, Moss SJ, Pangalos MN. 2000. $GABA_B$ receptors: a new paradigm in G protein signaling. Mol Cell Neurosci 16:296–312.

Dale LB, Bhattacharya M, Anborgh PH, Murdoch B, Bhatia M, Nakanishi S, Ferguson SS. 2000. G protein-coupled receptor kinase-mediated desensitization of metabotropic glutamate receptor 1A protects against cell death. J Biol Chem 275:38213–38220.

De Bartolomeis A, Iasevoli F. 2003. The homer family and the signal transduction system at glutamatergic postsynaptic density: potential role in behavior and pharmacotherapy. Psychopharmacol Bull 37:51–83.

DeLong MR. 1990. Primate models of movement disorders of basal ganglia origin. Trends Neurosci 13:281–285.

Dingledine R, Borges K, Bowie D, Traynelis SF. 1999. The glutamate receptor ion channels. Pharmacol Rev 51:7–61.

Doherty J, Dingledine R. 2003. Functional interactions between cannabinoid and metabotropic glutamate receptors in the central nervous system. Curr Opin Pharmacol 3:46–53.

Dournaud P, Boudin H, Schonbrunn A, Tannenbaum GS, Beaudet A. 1998. Interrelationships between somatostatin sst2A receptors and somatostatin-containing axons in rat brain: evidence for regulation of cell surface receptors by endogenous somatostatin. J Neurosci 18:1056–1071.

Ferraguti F, Conquet F, Corti C, Grandes P, Kuhn R, Knopfel T. 1998. Immunohistochemical localization of the mGluR1beta metabotropic glutamate receptor in the adult rodent forebrain: evidence for a differential distribution of mGluR1 splice variants. J Comp Neurol 400:391–407.

Gracy KN, Svingos AL, Pickel VM. 1997. Dual ultrastructural localization of mu-opioid receptors and NMDA-type glutamate receptors in the shell of the rat nucleus accumbens. J Neurosci 17:4839–4848.

Hanson JE, Smith Y. 1999. Group I metabotropic glutamate receptors at GABAergic synapses in monkeys. J Neurosci 19:6488–6496.

Hanson JE, Smith Y. 2002. Subcellular distribution of high-voltage-activated calcium channel subtypes in rat globus pallidus neurons. J Comp Neurol 442:89–98.

Hoffpauir BK, Gleason EL. 2002. Activation of mGluR5 modulates GABA(A) receptor function in retinal amacrine cells. J Neurophysiol 88:1766–1776.

Houamed KM, Kuijper JL, Gilbert TL, Haldeman BA, O'Hara PJ, Mulvihill ER, Almers W, Hagen FS. 1991. Cloning, expression, and gene structure of a G protein-coupled glutamate receptor from rat brain. Science 252:1318–1321.

Hubert GW, Paquet M, Smith Y. 2001. Differential subcellular localization of mGluR1a and mGluR5 in the rat and monkey substantia nigra. J Neurosci 21:1838–1847.

Iacovelli L, Salvatore L, Capobianco L, Picascia A, Barletta E, Storto M, Mariggio S, Sallese M, Porcellini A, Nicoletti F, De Blasi A. 2003. Role of G protein-coupled receptor kinase 4 and β-arrestin 1 in agonist-stimulated metabotropic glutamate receptor 1 internalization and ac-

tivation of mitogen-activated protein kinases. J Biol Chem 278:12433–12442.

Jensen AM, Chiu SY. 1993. Expression of glutamate receptor genes in white matter: developing and adult rat optic nerve. J Neurosci 13: 1664–1675.

Jonas P, Bischofberger J, Sandkuhler J. 1998. Corelease of two fast neurotransmitters at a central synapse. Science 281:419–424.

Jones KA, Borowsky B, Tamm JA, Craig DA, Durkin MM, Dai M, Yao WJ, Johnson M, Gunwaldsen C, Huang LY, Tang C, Shen Q, Salon JA, Morse K, Laz T, Smith KE, Nagarathnam D, Noble SA, Branchek TA, Gerald C. 1998. GABA(B) receptors function as a heteromeric assembly of the subunits GABA(B)R1 and GABA(B)R2. Nature 396:674–679.

Kaupmann K, Huggel K, Heid J, Flor PJ, Bischoff S, Mickel SJ, McMaster G, Angst C, Bittiger H, Froestl W, Bettler B. 1997. Expression cloning of GABA(B) receptors uncovers similarity to metabotropic glutamate receptors. Nature 386:239–246.

Kaupmann K, Malitschek B, Schuler V, Heid J, Froestl W, Beck P, Mosbacher J, Bischoff S, Kulik A, Shigemoto R, Karschin A, Bettler B. 1998. GABA(B)-receptor subtypes assemble into functional heteromeric complexes. Nature 396:683–687.

Kuwajima M, Philpot KB, Paré J-F, Smith Y. 2001. Subcellular localization of group I metabotropic glutamate receptors in the monkey subthalamic nucleus. Soc Neurosci Abstr 290.12.

Kuwajima M, Hubert GW, Smith Y. 2002. Subcellular and subsynaptic localization of group I metabotropic glutamate receptors in the subthalamic nucleus of normal animals and animal models of Parkinson's disease. 4th International Meeting on Metabotropic Glutamate Receptors, Taormina, Italy. Neuropharmacology 43:293.

Limousin P, Pollak P, Benazzouz A, Hoffmann D, Broussolle E, Perret JE, Benabid AL. 1995. Bilateral subthalamic nucleus stimulation for severe Parkinson's disease. Mov Disord 10:672–674.

Lujan R, Nusser Z, Roberts JD, Shigemoto R, Somogyi P. 1996. Perisynaptic location of metabotropic glutamate receptors mGluR1 and mGluR5 on dendrites and dendritic spines in the rat hippocampus. Eur J Neurosci 8:1488–1500.

Lujan R, Roberts JD, Shigemoto R, Ohishi H, Somogyi P. 1997. Differential plasma membrane distribution of metabotropic glutamate receptors mGluR1 alpha, mGluR2 and mGluR5, relative to neurotransmitter release sites. J Chem Neuroanat 13:219–241.

Mailleux P, Vanderhaeghen JJ. 1992. Distribution of neuronal cannabinoid receptor in the adult rat brain: a comparative receptor binding radioautography and in situ hybridization histochemistry. Neuroscience 48:655–668.

Marino MJ, Wittmann M, Bradley SR, Hubert GW, Smith Y, Conn PJ. 2001. Activation of group I metabotropic glutamate receptors produces a direct excitation and disinhibition of GABAergic projection neurons in the substantia nigra pars reticulata. J Neurosci 21:7001–7012.

Marino MJ, Awad-Granko H, Ciombor KJ, Conn PJ. 2002. Haloperidol-induced alteration in the physiological actions of group I mGlus in the subthalamic nucleus and the substantia nigra pars reticulata. Neuropharmacology 43:147–159.

Masu M, Tanabe Y, Tsuchida K, Shigemoto R, Nakanishi S. 1991. Sequence and expression of a metabotropic glutamate receptor. Nature 349:760–765.

Minakami R, Katsuki F, Sugiyama H. 1993. A variant of metabotropic glutamate receptor subtype 5: an evolutionally conserved insertion with no termination codon. Biochem Biophys Res Commun 194:622–627.

Mundell SJ, Matharu AL, Pula G, Roberts PJ, Kelly E. 2001. Agonist-induced internalization of the metabotropic glutamate receptor 1a is arrestin- and dynamin-dependent. J Neurochem 78:546–551.

Nakanishi S. 1992. Molecular diversity of glutamate receptors and implications for brain function. Science 258:597–603.

Nusser Z, Mulvihill E, Streit P, Somogyi P. 1994. Subsynaptic segregation of metabotropic and ionotropic glutamate receptors as revealed by immunogold localization. Neuroscience 61:421–427.

Paquet M, Smith Y. 2003. Group I metabotropic glutamate receptors in the monkey striatum: subsynaptic association with glutamatergic and dopaminergic afferents. J Neurosci 23:7659–7669.

Parpura V, Basarsky TA, Liu F, Jeftinija K, Jeftinija S, Haydon PG. 1994. Glutamate-mediated astrocyte-neuron signalling. Nature 369:744–747.

Petralia RS, Wang YX, Singh S, Wu C, Shi L, Wei J, Wenthold RJ. 1997. A monoclonal antibody shows discrete cellular and subcellular localizations of mGluR1 alpha metabotropic glutamate receptors. J Chem Neuroanat 13:77–93.

Petralia RS, Wang YX, Sans N, Worley PF, Hammer JA 3rd, Wenthold RJ. 2001. Glutamate receptor targeting in the postsynaptic spine involves mechanisms that are independent of myosin Va. Eur J Neurosci 13: 1722–1732.

Pierce KL, Lefkowitz RJ. 2001. Classical and new roles of beta-arrestins in the regulation of G-protein-coupled receptors. Nat Rev Neurosci 2:727–733.

Poisik OV, Mannaioni G, Traynelis S, Smith Y, Conn PJ. 2003. Distinct functional roles of the metabotropic glutamate receptors 1 and 5 in the rat globus pallidus. J Neurosci 23:122–130.

Reichelt W, Knopfel T. 2002. Glutamate uptake controls expression of a slow postsynaptic current mediated by mGluRs in cerebellar Purkinje cells. J Neurophysiol 87:1974–1980.

Rouse ST, Marino MJ, Bradley SR, Awad H, Wittmann M, Conn PJ. 2000. Distribution and roles of metabotropic glutamate receptors in the basal ganglia motor circuit: implications for treatment of Parkinson's disease and related disorders. Pharmacol Ther 88:427–435.

Sandler R, Smith AD. 1991. Coexistence of GABA and glutamate in mossy fiber terminals of the primate hippocampus: an ultrastructural study. J Comp Neurol 303:177–192.

Sato F, Lavallee P, Levesque M, Parent A. 2000. Single-axon tracing study of neurons of the external segment of the globus pallidus in primate. J Comp Neurol 417:17–31.

Shink E, Smith Y. 1995. Differential synaptic innervation of neurons in the internal and external segments of the globus pallidus by the GABA- and glutamate-containing terminals in the squirrel monkey. J Comp Neurol 358:119–141.

Shink E, Bevan MD, Bolam JP, Smith Y. 1996. The subthalamic nucleus and the external pallidum: two tightly interconnected structures that control the output of the basal ganglia in the monkey. Neuroscience 73:335–357.

Silva GA, Theriault E, Mills LR, Pennefather PS, Feeney CJ. 1999. Group I and II metabotropic glutamate receptor expression in cultured rat spinal cord astrocytes. Neurosci Lett 263:117–120.

Sloviter RS, Dichter MA, Rachinsky TL, Dean E, Goodman JH, Sollas AL, Martin DL. 1996. Basal expression and induction of glutamate decarboxylase and GABA in excitatory granule cells of the rat and monkey hippocampal dentate gyrus. J Comp Neurol 373:593–618.

Smith Y, Bevan MD, Shink E, Bolam JP. 1998. Microcircuitry of the direct and indirect pathways of the basal ganglia. Neuroscience 86:353–387.

Smith Y, Charara A, Paquet M, Kieval JZ, Pare JF, Hanson JE, Hubert GW, Kuwajima M, Levey AI. 2001. Ionotropic and metabotropic GABA and glutamate receptors in primate basal ganglia. J Chem Neuroanat 22:13–42.

Tempia F, Miniaci MC, Anchisi D, Strata P. 1998. Postsynaptic current mediated by metabotropic glutamate receptors in cerebellar Purkinje cells. J Neurophysiol 80:520–528.

Testa CM, Friberg IK, Weiss SW, Standaert DG. 1998. Immunohistochemical localization of metabotropic glutamate receptors mGluR1a and mGluR2/3 in the rat basal ganglia. J Comp Neurol 390:5–19.

Valenti O, Conn PJ, Marino MJ. 2002. Distinct physiological roles of the Gq-coupled metabotropic glutamate receptors co-expressed in the same neuronal populations. J Cell Physiol 191:125–137.

Walker MC, Ruiz A, Kullmann DM. 2001. Monosynaptic GABAergic signaling from dentate to CA3 with a pharmacological and physiological profile typical of mossy fiber synapses. Neuron 29:703–715.

Wang XS, Ong WY, Lee HK, Huganir RL. 2000. A light and electron microscopic study of glutamate receptors in the monkey subthalamic nucleus. J Neurocytol 29:743–754.

White JH, Wise A, Main MJ, Green A, Fraser NJ, Disney GH, Barnes AA, Emson P, Foord SM, Marshall FH. 1998. Heterodimerization is required for the formation of a functional GABA(B) receptor. Nature 396:679–682.

Wilkin GP, Marriott DR, Cholewinski AJ. 1990. Astrocyte heterogeneity. Trends Neurosci 13:43–46.

Winder DG, Conn PJ. 1996. Roles of metabotropic glutamate receptors in glial function and glial-neuronal communication. J Neurosci Res 46: 131–137.

Xiao B, Tu JC, Worley PF. 2000. Homer: a link between neural activity and glutamate receptor function. Curr Opin Neurobiol 10:370–374.

Yung KK, Bolam JP, Smith AD, Hersch SM, Ciliax BJ, Levey AI. 1995. Immunocytochemical localization of D1 and D2 dopamine receptors in the basal ganglia of the rat: light and electron microscopy. Neuroscience 65:709–730.